2009

Sulfur Dioxide Crossover during the Production of Hydrogen and Sulfuric Acid in a PEM Electrolyzer

John A. Staser
University of South Carolina - Columbia

John W. Weidner
University of South Carolina - Columbia, weidner@engr.sc.edu

Publication Info

Journal of the Electrochemical Society, 2009, pages B836-B841.

Publisher's link: http://dx.doi.org/10.1149/1.3129444
DOI: 10.1149/1.3129444

Journal of The Electrochemical Society, **156** (7) B836-B841 (2009)
0013-4651/2009/156(7)/B836/6/$25.00 © The Electrochemical Society

Sulfur Dioxide Crossover during the Production of Hydrogen and Sulfuric Acid in a PEM Electrolyzer

John A. Staser[*,z] **and John W. Weidner**[**,z]

Center for Electrochemical Engineering, Department of Chemical Engineering, University of South Carolina, Columbia, South Carolina 29208, USA

A proton exchange membrane (PEM) electrolyzer has been investigated as a viable system for the electrolysis step in the thermochemical conversion of sulfur dioxide to sulfuric acid for the large-scale production of hydrogen. Unfortunately, during operation, sulfur dioxide can diffuse from the anode to the cathode. This has several negative effects, including reduction to sulfur that could potentially damage the electrode, consumption of current that would otherwise be used for the production of hydrogen, introduction of oxygen and SO_2 to the hydrogen stream, and loss of sulfur to the cycle. However, proper water management can reduce or eliminate the transport of SO_2 to the cathode. Here we present model simulations and experimental data for the flux of SO_2 to the cathode as a function of current density and pressure differential across the membrane and show how water transport influences SO_2 crossover. Understanding SO_2 crossover is important in evaluating both the lifetime of the electrolyzer and membranes developed to limit SO_2 crossover.
 [DOI: 10.1149/1.3129444]

Manuscript submitted February 19, 2009; revised manuscript received April 10, 2009. Published May 19, 2009.

The hybrid sulfur process is being investigated as an efficient way to produce clean hydrogen on a large scale at efficiencies higher than water electrolysis.[1-17] In this thermochemical cycle, sulfuric acid is decomposed at high temperature (~850°C) to SO_2 and water, and the SO_2 is converted back to sulfuric acid in a proton exchange membrane (PEM) electrolyzer. Hence, the sulfur compounds are internally recycled, such that the overall process decomposes water into hydrogen and oxygen. We developed a gas-fed anode electrolyzer in which SO_2 is oxidized to H_2SO_4 via the following reaction[11,13,15,16]

$$SO_2 + 2H_2O \rightarrow H_2SO_4 + 2H^+ + 2e^- \quad E^0 = 0.158 \text{ V vs SHE} \qquad [1]$$

where SHE is the standard hydrogen electrode. The water required for Reaction 1 is supplied via the membrane from the cathode. The H^+ produced in Reaction 1 migrates through the membrane and reduces to hydrogen at the cathode

$$2H^+ + 2e^- \rightarrow H_2 \quad E^0 = 0 \text{ V vs SHE} \qquad [2]$$

We have successfully carried out Reactions 1 and 2 over a range of operating conditions (e.g., temperature, flow rate, and pressure differential) and design variations (i.e., catalyst loading and membrane type and thickness).[11,13,15,16]

We showed that water transport affected the electrolyzer performance (i.e., cell voltage) by controlling the sulfuric acid concentration at the anode. We in turn developed a model to predict water flux through the membrane as a function of membrane thickness, temperature, current density, and pressure differential.[16] We were able to accurately predict water management and correlate the resulting sulfuric acid concentration to the operating voltage.

Unfortunately, a detrimental side reaction occurs when SO_2 crosses the membrane to the cathode and is reduced to sulfur via the reaction

$$SO_2 + 4e^- \rightarrow S + O_2 \qquad [3]$$

The reduction of SO_2 to sulfur at the cathode consumes current that would otherwise be used for the production of hydrogen, introduces oxygen and SO_2 to the hydrogen stream that must be separated, and may increase cell resistance due to sulfur deposits in the electrode. SO_2 crossing the membrane, even if it is not reduced at the cathode via Reaction 3, is lost to the cycle and must be resupplied. For example, researchers at the Savannah River National Laboratory (SRNL) have observed a sulfur layer between the membrane and the cathode in the liquid-fed anode system, which leads to a significant delamination of the cathode from the membrane.[17] The delamination of the cathode is troubling because it occurs within 20 h of operation, and the long-term effects are not known. Hence, controlling the SO_2 crossover is critical to the long-term operation of the electrolyzer. Therefore, we have developed a model to quantify the SO_2 crossover and simulate how it is influenced by water transport.

Experimental

The experimental setup was similar to that reported in previous papers.[15,16] The cell was the standard 10 cm^2 cell from Fuel Cell Technologies, Inc. The reactants and products were passed through Kynar plates instead of the aluminum end plates. The cell was sandwiched between the aluminum end plates. The temperature was maintained by the use of heating rods inserted into the aluminum end plates.

Liquid water was fed to the cathode by a metering pump, and gaseous SO_2 was fed to the anode. The cell was maintained at 80°C, and the water was heated to 88°C before being fed to the cathode. The membrane electrode assembly (MEA) contained Pt black with a loading of 1.5 mg/cm^2 on each side of the membrane. The membranes were either N212 or N115 (2 and 5 mil thicknesses, respectively). The SO_2 flow rate was maintained so that the conversion rate at the anode was 20%. We have shown previously, however, that conversion and catalyst loading have little effect on the electrolyzer performance.[15]

A pressure differential was maintained across the membrane by the use of a globe valve on the exit stream of the cathode. The gaseous feed stream to the anode was maintained at 101 kPa. The electrolyzer was run at a constant current and different pressure differentials, and energy dispersive X-ray (EDX) elemental analysis was performed on the anode and cathode to determine the buildup of sulfur in the cathode.

The electrochemical monitoring technique[18] was used to determine the diffusion coefficient and the solubility of SO_2 in Nafion. The membrane pressure differential was initially maintained at $\Delta P = 0$ kPa, N_2 was fed to the gas side, and a voltage of 0.31 V was applied. The gas was then switched to SO_2, with the cell voltage maintained at 0.31 V. The SO_2 crossing the membrane was oxidized to sulfuric acid on the liquid water side and hydrogen evolved on the gaseous SO_2 side. The slight increase in the water flux toward the gaseous SO_2 side due to the electro-osmotic drag was considered negligible for the analysis. The measured limiting current was a result of the mass-transfer-limited flux of SO_2 across the membrane, with the transient data useful for determining the diffusion coefficient and solubility.

* Electrochemical Society Student Member.
** Electrochemical Society Active Member.
z E-mail: staser@engr.sc.edu; weidner@engr.sc.edu

The water uptake of the membrane was measured by equilibrating the membrane with sulfuric acid and measuring the weight change. The weight change was attributed to the absorption of water by the membrane. The experiment was carried out over a range of temperatures from 40 to 90°C.

EDX elemental analysis was performed on MEAs after testing. A cross section of the MEA was imaged using scanning electron microscopy (SEM), and the sulfur content of the anode and cathode was measured using elemental analysis to determine the amount of sulfur reduced at the cathode during operation. The gas diffusion layers were removed prior to imaging.

Model Development

For a cell operating under conditions to drive Reactions 1 and 2, the water transport model was developed in our previous paper,[16] with the water flux equation given by

$$N_w = \frac{\rho_M}{M_M \delta_M}\int_{\lambda_a}^{\lambda_c} D_w d\lambda - \frac{\xi \lambda_a i_{H_2SO_4}}{\lambda_c F} + \frac{P_M}{\delta_M}(P_c - P_a) \qquad [4]$$

A list of parameter values and the resulting water flux, N_w, from Eq. 4 as a function of current, pressure differential, and membrane thickness has been given previously.[16] The pre-exponential factors in the diffusion coefficient

$$D_w = A_1\lambda(1 + e^{-0.28\lambda})\exp\left[\frac{-2436}{T}\right] \quad (\text{for } 0 < \lambda \leq 3) \quad [5a]$$

$$D_w = A_2\lambda(1 + 161e^{-\lambda})\exp\left[\frac{-2436}{T}\right] \quad (\text{for } 3 < \lambda \leq 17) \quad [5b]$$

have been found to be weak functions of temperature. Because the temperature dependence was small, the same value was used at all temperatures (i.e., $A_1 = 2.2 \times 10^{-3}$ cm^2/s and $A_2 = 8.3 \times 10^{-4}$ cm^2/s).

The water content of the membrane, λ, was measured as a function of sulfuric acid concentration by equilibrating the membrane with a solution of sulfuric acid and measuring the change in weight. The weight gain was attributed to the water uptake, and at 80°C the expression was found to be

$$\lambda_a = 123.8y_w^3 - 224.01y_w^2 + 134.14y_w - 16.35 \qquad [6]$$

where a_w is the activity of water. Our previous paper[3] used an expression for water uptake in the vapor phase at 30°C.[19] Water uptake was not a strong function of temperature; Eq. 6 was used at all temperatures. Once N_w is obtained, Eq. 4 can be used to obtain the λ profile through the membrane [i.e., $\lambda(x)$].

The water flux, N_w, and the λ profile, both found from Eq. 4, can be used to calculate the flux of SO_2 via the following equation

$$N_{SO_2} = \frac{C_{SO_2}M_M}{\lambda\rho_M}N_w - D_{SO_2}\frac{dC_{SO_2}}{dx} \qquad [7]$$

with the boundary conditions $C_{SO_2} = C^*_{SO_2}$ at $x = 0$ (gas anode side) and $C_{SO_2} = 0$ at $x = \delta_M$ (liquid cathode side). The flux of SO_2 is a combination of convective transport with the water toward the anode (first term on the right) and diffusional flux to the cathode due to a concentration gradient (second term on the right).

When the water flux obtained via Eq. 4 is zero (i.e., no pressure differential, open-circuit conditions) Eq. 7 reduces to the following form

$$N_{SO_2} = -D_{SO_2}\frac{dC_{SO_2}}{dx} \qquad [8]$$

Equation 8 is Fick's first law. Combining Eq. 8 with the transient material balance gives Fick's second law

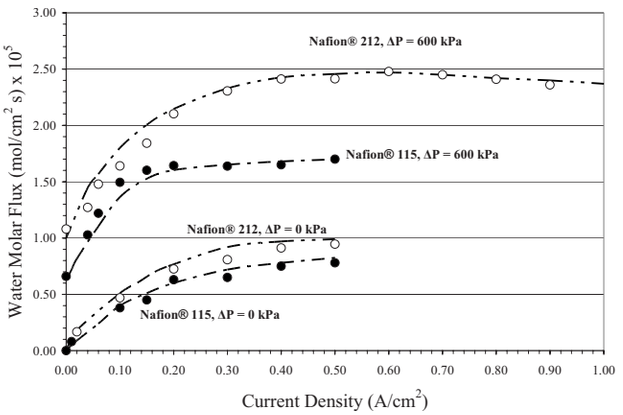

Figure 1. Model predictions from Eq. 4 (lines) and experimental data (points: N115, ●; N212, ○) for the molar flux of water as a function of current density at different Δ*P*. The cell temperature was 80°C.

$$\frac{\partial C_{SO_2}(x,t)}{\partial t} = -D_{SO_2}\frac{\partial^2 C_{SO_2}(x,t)}{\partial x^2} \qquad [9]$$

Equation 9 can be solved with the following initial and boundary conditions[18]

$$C_{SO_2} = 0 \quad @ \quad t = 0 \qquad [10a]$$

$$C_{SO_2} = C^*_{SO_2} \quad @ \quad x = 0 \qquad [10b]$$

$$C_{SO_2} = 0 \quad @ \quad x = \delta_M \qquad [10c]$$

to render the following equation for the SO_2 crossover current as a function of time

$$i_{SO_2}(t) = \frac{2FD_{SO_2}C^*_{SO_2}}{\delta_M}\left(\frac{2}{\sqrt{\pi\tau}}\sum_{j=0}^{\infty}\exp\left[-\frac{(2j+1)^2}{4\tau}\right]\right) \qquad [11]$$

The electrochemical monitoring technique is used to calculate the parameters D_{SO_2} and $C^*_{SO_2}$ via a least-squares fit method at conditions under which Eq. 8 is valid (i.e., $N_w = 0$).[18] The current achieved during the electrochemical monitoring technique is small enough that water flux due to electro-osmotic drag is assumed to be negligible. The τ in Eq. 11 is defined as

$$\tau = \frac{tD_{SO_2}}{\delta_M^2} \qquad [12]$$

The SO_2 flux is converted to a crossover current density by the following relationship

$$i_{SO_2} = 2FN_{SO_2} \qquad [13]$$

Results and Discussion

As given by Eq. 7, a SO_2 crossover is a strong function of the water transport in the membrane. Thus, any discussion of SO_2 crossover must begin with an investigation of water flux in the membrane. Solving Eq. 4, along with parameters given previously,[16] gives the flux of water through the membranes as a function of current density at differential pressures of 600 and 0 kPa; these values are shown in Fig. 1. The two pressure differentials were chosen to highlight the extreme cases of high and low pressure differentials. The points are data and the lines are model predictions. For the conditions shown in Fig. 1, the water flux to the anode increases with current density up to approximately 0.5 A/cm^2. At current densities higher than 0.5 A/cm^2, the electro-osmotic drag to the cathode is high enough to offset the diffusion and pressure-driven flux to the anode. Under these conditions, the water flux to

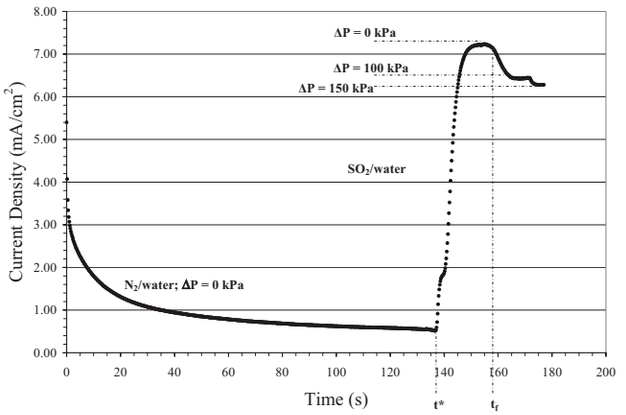

Figure 2. Electrochemical monitoring technique on N115. The cell voltage and temperature were 0.31 V and 80°C, respectively. The limiting current is the SO_2 crossover current density, i_{SO_2}.

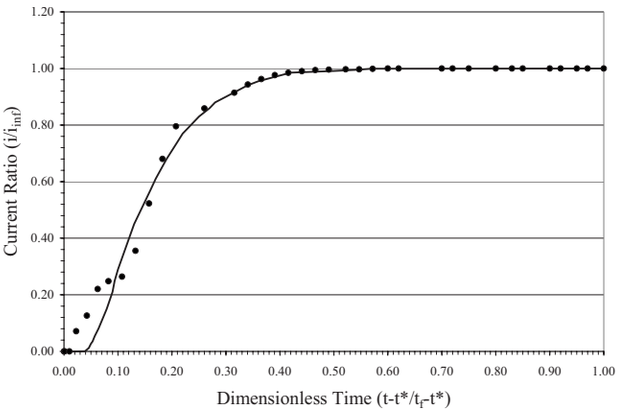

Figure 3. Comparison of experimental data (points) and the model using least-squares fit (line) of the transient region. The resulting fit, obtained by the least-squares method, yielded values D_{SO_2} and $C^*_{SO_2}$ as model parameters.

the anode begins to decrease. The model predicts a decrease in the water flux to the anode at current densities above 0.5 A/cm^2 for the $\Delta P = 0$ kPa case. However, due to the more concentrated sulfuric acid[16,20] at $\Delta P = 0$ kPa, the electrolyzers could not be run past 0.5 A/cm^2.

The water flux values shown in Fig. 1 are used in conjunction with D_{SO_2} and $C^*_{SO_2}$ values obtained from the electrochemical monitoring technique and Eq. 13 to determine the SO_2 flux via Eq. 7. The data obtained from the electrochemical monitoring technique for N115 are shown in Fig. 2. Initially, N_2 is sent to the gas side (cathode) and liquid water is sent to the other (anode), with $\Delta P = 0$ kPa. At time $t = 0$ s, a step voltage of 0.31 V is applied. The current density immediately increases due to double-layer charging and then begins to decay. Once the current reaches the steady-state value at $t = t^*$, the gas at the cathode is switched to SO_2. The voltage at the anode ($\sim$0.31 V) is such that any SO_2 crossing the membrane to the water side is oxidized to H_2SO_4. This operation is opposite of normal electrolyzer operation; during the electrochemical monitoring technique, the water side serves as the anode, and SO_2 crossing the membrane is oxidized to H_2SO_4. Thus, the anode voltage must be above 0.158 V, and the limiting current indicates that all SO_2 crossing the membrane is oxidized. The limiting current density reached at t_f is the SO_2 crossover current, i_{SO_2}. The membrane pressure differential, ΔP, is subsequently increased to 100 kPa and then to 150 kPa, resulting in a lower value for i_{SO_2}. The decrease in i_{SO_2} as ΔP increases is indicative of the convective flux of SO_2 toward the gas side due to water flux.

The portion of the data in Fig. 2 where the N_2 feed was switched to SO_2 at $\Delta P = 0$ kPa is shown in Fig. 3. The time axis, starting with the switch at t^*, has been normalized with respect to t_f. The SO_2 crossover current density, i_{SO_2}, has been normalized with respect to the limiting current density. The transient data in which the SO_2 crossover current density increased to the limiting value were used in a least-squares model[18] to determine D_{SO_2} and $C^*_{SO_2}$ via Eq. 11. The diffusion coefficient at 80°C was $D_{SO_2} = 2.86 \times 10^{-6}$ cm^2/s, and the solubility in Nafion was $C^*_{SO_2} = 1.58 \times 10^{-4}$ mol/cm^3.

Equation 11 was derived assuming $N_w = 0$, which is true for the data shown between t^* and t_f in Fig. 2 and 3. When a pressure differential is applied, $N_w \neq 0$, and Eq. 11 is no longer valid. However, the steady-state current is still a measure of the steady-state SO_2 crossover occurring during electrolyzer operation. Therefore, the steady-state current was measured for N115 and N212 at various membrane pressure differentials. These data are shown in Fig. 4 along with the model predictions for i_{SO_2} obtained via Eq. 7 and 13. The data and model predictions indicate that i_{SO_2} is higher for N212 than for N115. For example, at $\Delta P = 400$ kPa, i_{SO_2} is approximately 11.1 mA/cm^2 for N212 and 4.4 mA/cm^2 for N115. The decrease in i_{SO_2} observed in the thicker N115 membrane is due to the lower diffusion term in the convection-diffusion equation (Eq. 7).

Another trend is observed in Fig. 4, namely, that as ΔP increases, i_{SO_2} decreases. The decrease in i_{SO_2} as the pressure differential increases is the same trend observed during the electrochemical monitoring technique in Fig. 2. One concludes that as the pressure differential is increased (and hence the water flux to the anode due to Eq. 4), the SO_2 crossover decreases due to its solubility in water (i.e., the convective term in Eq. 7 works to counter diffusion).

The solubility and diffusion coefficient of SO_2 as functions of temperature are shown in Fig. 5 for N115. The data were obtained by the electrochemical monitoring technique in the same manner described above. As expected, the solubility of SO_2 is higher at lower temperatures.[21] For example, we have indicated in the discussion of the electrochemical monitoring technique in Fig. 2 and 3 that at 80°C, $C^*_{SO_2} = 1.58 \times 10^{-4}$ mol/cm^3. The solubility increases as the temperature decreases; at 50°C the solubility $C^*_{SO_2} = 4.00 \times 10^{-4}$ mol/cm^3. The diffusion coefficient increases with temperature. The solubility and diffusion coefficient for N212 at 80°C are shown for comparison and are within the experimental error of those

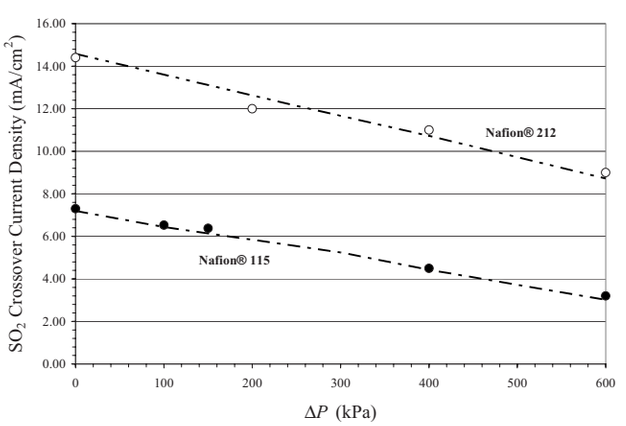

Figure 4. SO_2 crossover current density as a function of membrane ΔP. The lines are the model predictions and the points (N115, ●; N212, ○) are experimental data. The temperature was 80°C.

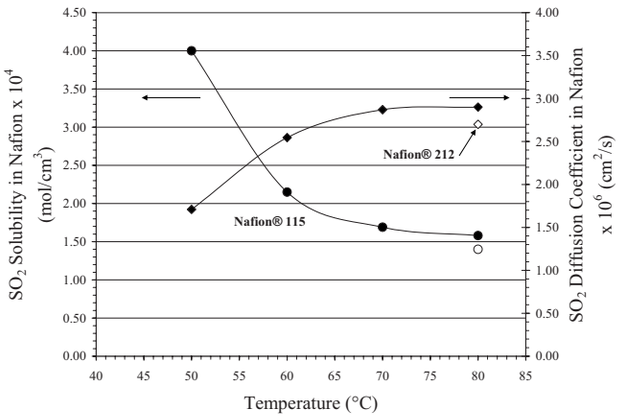

Figure 5. Solubility of SO_2 in Nafion as a function of temperature. The points (N115, ● and ♦; N212, ○ and ◇) are data and the lines are smooth curve fits to the data. The membrane pressure differential was $\Delta P = 0$ kPa.

values reported for N115. It was determined that the solubility of SO_2 in a hydrated Nafion membrane was within 10% of the reported value for the solubility in water.[21] This result is consistent with our understanding of a hydrated Nafion membrane, in which as many as 20 moles of water can exist for each mole of sulfonate group.

We have shown that at the very low current densities (i.e., <0.02 A/cm^2) achieved in the electrochemical monitoring technique, increasing the membrane pressure differential, ΔP, leads to a decrease in the SO_2 crossover current density, i_{SO_2}. This is due to the increased water flux to the anode observed in Fig. 1, which increases the convective term in Eq. 7 and offsets diffusion. In addition to increasing water flux to the anode by increasing ΔP, one can also increase water flux by increasing the electrolyzer current density, as shown in Fig. 1. One would expect that, just like increasing ΔP lowers i_{SO_2}, increasing the electrolyzer current density should also lower i_{SO_2}.

This trend is observed in Fig. 6. As the current density increases (increasing the water flux to the anode), the convection term in Eq. 7 becomes larger, continually offsetting the diffusion term. As a result, the SO_2 crossover current density, i_{SO_2}, decreases. The decrease in i_{SO_2} as the current density increases can be quite dramatic, and i_{SO_2} actually goes to zero for N115 at sufficiently high ΔP and current density.

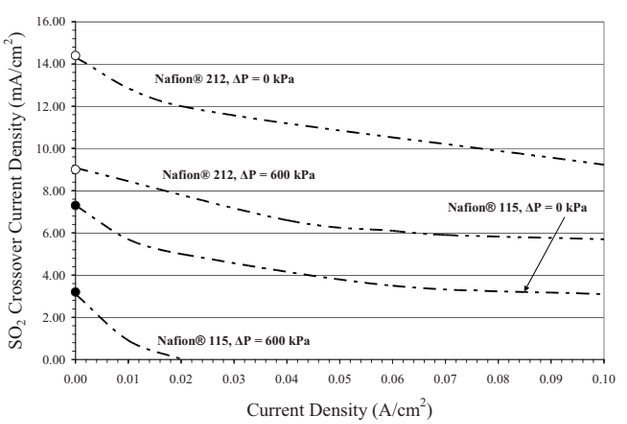

Figure 6. SO_2 crossover current density. The cell temperature was 80°C. The SO_2 flux decreases as current density increases due to the increase in the water flux with current density. The lines are model predictions from Eq. 7. At sufficiently high ΔP and current density, it is observed that SO_2 crossover can be prevented.

Table I. Ratio of sulfur at the cathode and anode after operation at various conditions measured by EDX elemental analysis for N115. The trend indicates that SO_2 crossover can be prevented if ΔP and the current density are sufficiently high.

	Case 1	Case 2	Case 3	Case 4
Current density (A/cm^2)	0.25	0.10	0.10	0.02
Time (h)	15	16	8/4	100
ΔP (kPa)	600	0	600/0	200
SO_2 crossover (mol)	0	9.55×10^{-3}	2.41×10^{-3}	5.60×10^{-2}
Sulfur deposited in cathode (mol)	0	3.13×10^{-5}	8.92×10^{-6}	1.96×10^{-4}
Sulfur reduced (%)	0	0.33	0.37	0.35

Unfortunately, it is not possible to experimentally measure the SO_2 crossover current, i_{SO_2}, while the electrolyzer is operated under load. For this reason, the only experimental data presented in Fig. 6 are for the zero current case, which was taken from Fig. 4. However, these data do provide a quantitative agreement between the water flux and the SO_2 crossover. Therefore, it lends credibility to the values of the SO_2 crossover predicted under load from Eq. 4 and 7, and shown in Fig. 6. As a means to further estimate the SO_2 crossover under load and determine the extent of sulfur deposition via Reaction 3, sulfur deposition at the cathode was correlated with water flux predicted by the model by utilizing EDX elemental analysis. N115 membranes were run under several different conditions, and cross sections were taken of each membrane for EDX elemental analysis. The conditions, referred to as cases 1–4, are reported in Table I. Cases 1, 2, and 4 were run at a constant membrane pressure differential, ΔP, and current density for different lengths of time. Case 3 was run at a constant current density, but ΔP was changed at a point in the experiment.

EDX elemental analysis provides elemental weight percents in the anode and cathode. Because the mass of Pt in the electrodes is known, the total mass of the electrode can be determined from the weight percent data. The mass of sulfur in the electrodes is calculated from the sulfur weight percent via EDX and the total mass of the electrode. Because reduction of SO_2 to sulfur via Reaction 3 cannot occur at the anode, any sulfur in the anode is taken to exist due to the Nafion ionomer used as a binder. Hence, the sulfur content in the anode from EDX is taken as the background value. The additional sulfur found in the cathode after electrolyzer operation is assumed to be from the reduction of SO_2 crossing the membrane to sulfur via Reaction 3.

Investigating case 1, the model predicts no SO_2 crossover under these conditions, as shown in Fig. 6. EDX elemental analysis has shown negligible difference in the sulfur content of the anode and cathode, indicating no SO_2 crossover or reduction to sulfur in the cathode.

For case 2, the model predicts SO_2 crossover current density of $i_{SO_2} = 3.2$ mA/cm^2, corresponding to a total sulfur crossover during the 16 h run of 9.55×10^{-3} mol. Under the conditions of case 2, 3.13×10^{-5} mol of sulfur were reduced at the cathode. Thus, only about 0.33% of the sulfur crossing the membrane was reduced to elemental sulfur at the cathode.

A similar analysis was performed for cases 3 and 4, with very similar results, as shown in Table I. Thus, approximately 0.35% of the sulfur crossing the membrane is reduced to elemental sulfur at the cathode, regardless of operating conditions. The rest of the sulfur, in the form of SO_2, is swept out of the cathode compartment with the water. The percent of sulfur crossing the membrane, in addition to being small, is almost the same at each condition tested. Therefore, reducing the amount of SO_2 crossing the membrane should result in a lower rate of sulfur reduction at the cathode.

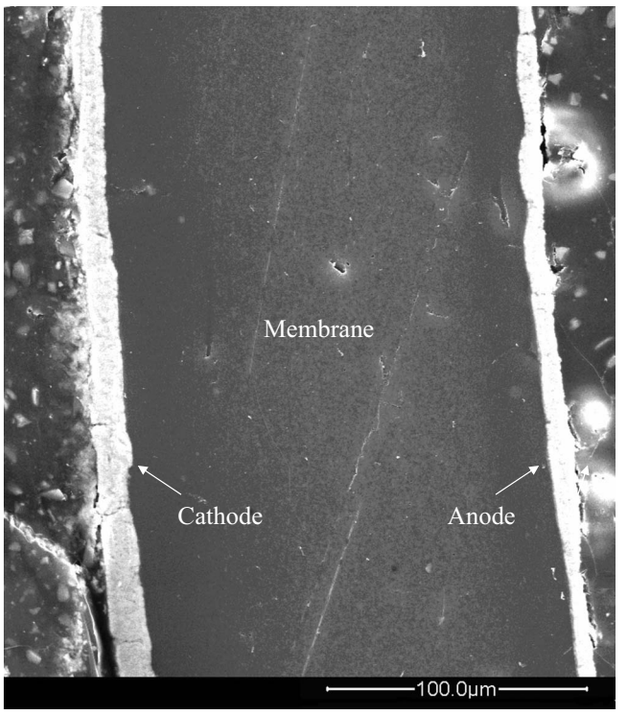

Figure 7. SEM image of N115 run at 0.02 A/cm^2 for 100 h with ΔP = 200 kPa. SO_2 crosses the membrane from the anode to the cathode via a concentration gradient and reduces to sulfur inside the cathode via Reaction 3.

To visualize the EDX analysis, the membranes were imaged by SEM under the conditions of cases 1–4. A representative sample (case 4) is shown in Fig. 7. All cases showed similar SEM images. The white vertical band at the right of Fig. 7 is the anode. The Nafion membrane (N115) is to the left of the anode, followed by the cathode. A sulfur layer has built up to the left of the cathode. The gas diffusion layers were removed from the MEA prior to imaging by SEM, and it is not clear to what extent that sulfur reduction occurs inside the gas diffusion layer. EDX elemental analysis has shown that approximately 0.35% of SO_2 crossing the membrane reduces to sulfur at the cathode. However, SEM images have not shown a visual change in the cathode after sulfur reduction. Comparing EDX elemental analysis results with the SEM image in Fig. 7 indicates that sulfur reduces inside the porous cathode until the pores are filled with sulfur. After this occurs, it appears that sulfur begins to build up outside of the cathode. However, we have not seen a delamination of the cathode, with a sulfur layer between the cathode and the membrane, as reported by SRNL.[17]

Besides changing the composition of the cathode and potentially building up into the gas diffusion layer, sulfur deposition via Reaction 3 consumes current that would ideally be used for the production of hydrogen. This serves to render the electrolyzer less efficient, but the current consumed by the reduction to sulfur is small enough that current efficiencies are still >99%. SO_2 crossing the membrane is lost to the sulfur cycle and must be added as fresh SO_2. The SO_2 crossing the membrane could also contaminate the H_2 product stream. The reduced sulfur at the cathode results in a compositional change of the electrode. It has not been shown, however, that changing the composition of the electrode over time results in significant voltage losses because the longest operation has only been for 100 h. It has been shown that the SO_2 crossover can be controlled by two means, namely, by increasing the current density and by increasing the pressure differential. Both methods increase the water flux to the anode, which increases the convective transport of SO_2 toward the anode.

Conclusions

The mechanism of the SO_2 crossover in the hybrid sulfur PEM electrolyzer has been investigated as a function of applied current, membrane thickness, and pressure differential. The SO_2 crossover is important because it could introduce SO_2 into the hydrogen stream, results in a loss of sulfur to the cycle, and can potentially reduce to sulfur upon reaching the cathode. This reduction has been shown by the SEM image and elemental analysis to change the composition of the cathode relative to the anode but has not been shown to significantly affect the cell voltage during a long-term operation. However, the current lifetime operation of the electrolyzer has reached 100 h; a longer lifetime testing is needed to fully understand the effect of sulfur reduction at the cathode.

We have shown that the extent of the reduction to elemental sulfur is approximately 0.35% of the sulfur crossing the membrane, indicating that reducing the SO_2 crossover can lead to a lower rate of reduction to elemental sulfur. We have shown that the SO_2 crossover to the cathode can be controlled by managing the water flux to the anode. Because SO_2 is soluble in water, the water flux to the anode contributes to the convective transport of SO_2 to the anode. We have shown that by increasing the current density or by increasing the pressure differential, one can limit the SO_2 crossover to the cathode, which prevents any change in the cathode catalyst due to sulfur reduction.

Acknowledgments

The authors thank the U.S. Department of Energy for funding this work (grant no. DE-FC07-06ID14752).

University of South Carolina assisted in meeting the publication costs of this article.

List of Symbols

C_i	concentration of species i, mol/cm^3
D_i	Fickian diffusion coefficient of species i, cm^2/s
E^0	standard reduction potential, V
F	Faraday's constant
i	current density, A/cm^2
M_M	molecular weight of membrane, g/mol
N_i	flux of species i, mol/cm^2 s
P_j	pressure in region j, kPa
P_M	membrane permeability, mol/cm s kPa
ΔP	pressure differential across the membrane ($P_c - P_a$), kPa
t	time, s
x	distance into membrane, cm
y_i	mole fraction of species i

Greek

δ_M	thickness of the catalyst coated membrane, cm
λ	water content of the membrane, mol H_2O/mol SO_3^-
λ_k	water content of the membrane at interface k, mol H_2O/mol SO_3^-
ξ	electro-osmotic drag coefficient, H^+/H_2O
ρ_M	density of Nafion, g/cm^3
τ	dimensionless time

Subscripts

a	anode
c	cathode
w	water

References

1. M. B. Gorensek, Model-Based Performance Comparison of Thermochemical Nuclear Hydrogen Processes, AIChE Spring 2005 Meeting, Session 73 presentation, April 11, 2005.
2. Department of Energy (DOE), Energy Information Administration, Hydrogen Use, Petroleum Consumption and Carbon Dioxide Emissions, Washington, DC (2008).
3. E. Varkaraki, N. Lymberopoulos, E. Zoulias, D. Guichardot, and G. Poli, *Int. J. Hydrogen Energy*, **32**, 1589 (2007).
4. Y. Shin, W. Park, J. Chang, and J. Park, *Int. J. Hydrogen Energy*, **32**, 1486 (2007).
5. J. S. Herring, J. E. O'Brien, C. M. Stoots, G. L. Hawkes, J. J. Hartvigsen, and M. Shahnam, *Int. J. Hydrogen Energy*, **32**, 440 (2007).
6. Nuclear Hydrogen, RRD Plan DRAFT, Department of Energy, Office of Nuclear Energy, Science and Technology, 2004.

7. Nuclear Hydrogen Initiative: Ten Year Program Plan, Office of Advanced Nuclear Research, DOE Office of Nuclear Energy, Science and Technology, March 2005.
8. A. Hauch, S. H. Jensen, S. Ramousse, and M. Mogensen, *J. Electrochem. Soc.*, **153**, A1741 (2006).
9. P. W. Lu, E. R. Garcia, and R. L. Ammon, *J. Appl. Electrochem.*, **11**, 347 (1981).
10. P. W. Lu and R. L. Ammon, *J. Electrochem. Soc.*, **127**, 2610 (1980).
11. P. Sivasubramanian, R. P. Ramasamy, F. J. Freire, C. E. Holland, and J. W. Weidner, *Int. J. Hydrogen Energy*, **32**, 463 (2007).
12. M. B. Gorensek and W. A. Summers, *Int. J. Hydrogen Energy*, doi: 10.1016/j.ijhydene.2008.06.049.
13. J. A. Staser, K. Norman, C. H. Fujimoto, M. A. Hickner, and J. W. Weidner, *J. Electrochem. Soc.*, **156**, B842 (2009).
14. F. Jomard, J. P. Feraud, and J. P. Caire, *Int. J. Hydrogen Energy*, **33**, 1142 (2008).
15. J. A. Staser, R. P. Ramasamy, P. Sivasubramanian, and J. W. Weidner, *Electrochem. Solid-State Lett.*, **10**, E17 (2007).
16. J. A. Staser and J. W. Weidner, *J. Electrochem. Soc.*, **156**, B16 (2009).
17. W. A. Summers, J. Steimke, T. Steeper, D. Hobbs, H. Colon-Mercado, and D. Herman, Hybrid Sulfur Thermochemical Process Development, DOE Hydrogen Program Report (2007).
18. A. T. Haug and R. E. White, *J. Electrochem. Soc.*, **147**, 980 (2000).
19. T. A. Zawodzinski, C. Derouin, S. Radzinski, R. J. Sherman, V. T. Smith, T. E. Springer, and S. Gottesfeld, *J. Electrochem. Soc.*, **140**, 1041 (1993).
20. M. B. Gorensek, J. A. Staser, T. G. Stanford, and J. W. Weidner, *Int. J. Hydrogen Energy*, Submitted.
21. R. E. Kirk and H. F. Mark, *Kirk-Othmer Encyclopedia of Chemical Technology*, Interscience, New York, (1963).